Pis'ma v ZhETF, vol. 95, iss. 6, pp. 317 – 322 © 2012 March 25

Anisotropic distributions of electrical currents in high-T_c grain-boundary junctions

M. Yu. Kupriyanov, M. M. Khapaev, Y. Y. Divin+, V. N. Gubankov+*

Lomonosov Moscow State University, Skobeltsyn Institute of Nuclear Physics, 119991 Moscow, Russia

**Peter Gruenberg Institute, Forschungszentrum Juelich, 52425 Juelich, Germany*

+Kotel'nikov Institute of Radio Engineering and Electronics of the RAS, 125009 Moscow, Russia

Submitted 14 February 2012

We developed a self-consistent method for calculations of spatial current distributions in high-T_c grain-boundary junctions. It is found that crystallographic anisotropy of high- T_c superconducting electrodes results in the effects, which previously were not taken into account for interpretations of experimental data. Among them is a significant redistribution of electrical currents in superconducting electrodes in the vicinity of a grain boundary. In particular in the case of [100]-tilt bicrystal junctions, this current redistribution results in a substantial focusing to the top or bottom part of a thickness of the grain boundary, depending on "roof"- or "valley"-type of the grain boundary. This redistribution is accompanied by generation of vortex currents around the grain boundary, which leads to selfbiasing of grain-boundary junctions by magnetic field nucleated by these vortex currents. It is shown that twinning or variation of geometrical shape of the high-T_c electrode may also result in intensive redistribution of electrical currents and nucleation of local magnetic fields inside a high-T_c superconducting electrodes.

A decisive role in electrical transport in high-T_c superconducting materials with anisotropic pairing, like cuprate superconductors [1, 2] and Fe-based compounds [3–6], belongs to grain boundaries (GB). Among a variety of possible crystallographical orientations of grains forming a boundary, the [001] tilt GB (see Fig. 1a) had

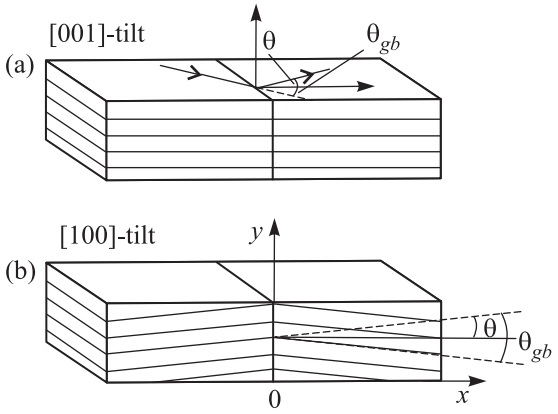

Fig. 1. Schematic diagram showing the crystallography of a [001]-tilt boundary (a), a [100]-tilt boundary (b)

been studied the most intensively with an emphases on the effect of order parameter symmetry and the mechanisms of charge transfer across the GB-interface [1, 2], [7–15].

Recently, [100]-tilt high-T_c GB-junctions with mutually tilted c-axis's (see Fig. 1b) have been fabricated [16–25] with an order of magnitude lower GB meandering and up to a threefold increase of the I_cR_n-values [16–19]. A complete antiphase correlation between low-frequency fluctuations of the resistance R_n and the critical current I_c has been observed in these junctions, thus showing that both quasiparticles and Cooper pairs flow directly through the same regions of the barrier [24]. In spite of intensive efforts, the mechanisms of electrical transport through grain boundaries in high-T_c superconductors are still far from understanding. This is true not only in respect of physics of conductivity of GB itself, but also in respect of influence of normal and supercurrent redistribution in the vicinity of GB on their properties.

It is well known that strong anisotropy of resistivity of high-T_c materials must be taken into account during interpretations of electrical data. A simple assumption that electrical resistivity of the material is proportional to the measured resistance with some coefficient of proportionality given by sample geometry may give an incorrect result [26–36].

The same must be obviously true for GB-junctions, since superconducting electrodes are anisotropic materials in both geometries presented in Fig. 1. Therefore, simply considering these GB-junctions as structures biased by homogeneously distributed current may also result in incorrect interpretations of data.

Previously the problem of electrodes anisotropy in high-T_c GB had been considered only for [100]-twist

GB [37] under assumption that the applied current is located in the vicinity of GB and flows along it. It had been shown that in this geometry the current flows in helical paths and provides appearance of inductance. It also generates the magnetic field components. Unfortunately, the problem considered in [37] is not applicable to a majority of experiments, where the current is applied in the direction normal to GB-interface and crystallographical orientations are either [001] or [100] tilt GB (see Fig. 1).

The goal of this study is to demonstrate that even in a nanowire composed from two single-crystalline high-T_c thin films separated by [100]-tilt GB, an assumption of a uniform distribution of the normal current over the film thickness, being natural for low-T_c junction, generally does not work and is valid only in the limit of extremely small conductivity of GB-interface.

To prove this statement, we consider a [100]-tilt GB shown in Fig. 1b. We suppose that it forms by two untwined single-crystalline blocks separated by GB, which characterized by a thickness L and an isotropic conductivity σ_B. Both the width w and thickness d_s of the blocks are assumed to be much smaller than effective London penetration depth. The conductivity of the blocks in c direction, σ_c, is taken to be 100 times smaller than that in ab plane, σ_a, which is actually in the case of the best single crystals of $YBa_2Cu_3O_{7-x}$ [38]. For simplicity, below we will not take into account the difference between σ_a and σ_b since it is much smaller than that between σ_c and σ_a. We assume also that the current leads located sufficiently far from GB so that the details of current injections does not influence on the spatial distribution of the current far from GB, which is assumed to be uniform in a cross section of the blocks.

Under these assumptions, the normal current distribution in the vicinity of GB can be found from the solution of Laplace equation for scalar potential φ. Inside the crystallographical blocks, it has the form

$$\frac{\partial^2\varphi}{\partial y^2}\sigma_{yy} + 2\sigma_{xy}\frac{\partial^2\varphi}{\partial y\partial x} + \sigma_{xx}\frac{\partial^2\varphi}{\partial x^2} = 0, \qquad (1)$$

where components of the conductivity tensor, σ_{xx}, σ_{yx}, and σ_{yy} relates to σ_c and σ_a by equations

$$\sigma_{xx} = \left(\sigma_a\cos^2\theta + \sigma_c\sin^2\theta\right), \qquad (2)$$

$$\sigma_{yy} = \left(\sigma_c\cos^2\theta + \sigma_a\sin^2\theta\right), \qquad (3)$$

$$\sigma_{yx} = \sigma_{xy} = (\sigma_c - \sigma_a)\cos\theta\sin\theta, \qquad (4)$$

and θ is the angle between x-axis and crystallographical axis a (see Fig. 1b).

GB is modeled either as a single interface having resistance, R, and area, $A = wd_s$, or as a layer, which is characterized by isotropic conductivity σ_B and thickness $L \ll d_s$. In the first case, it describes by the boundary conditions in the form

$$j_x(-0,y) = j_x(+0,y) = \frac{\varphi(+0,y) - \varphi(-0,y)}{Rwd_s}, \qquad (5)$$

where $R = L\sigma_B^{-1}$. These conditions provide the conservation of x component of the current density across the interface. If the boundary is completely transparent ($R = 0$), they are transformed to classical conditions of continuity for a component of the current density, normal to the interface, and potential:

$$j_x(-0,y) = j_x(+0,y), \quad \varphi(+0,y) = \varphi(-0,y). \qquad (6)$$

In the second interface model, we have used the boundary conditions (6) at $x = \pm L/2$.

Boundary conditions at free interfaces $-S \le x \le S$, $y = 0, d_s$,

$$j_y = \frac{\partial\varphi}{\partial y}\sigma_{yy} + \frac{\partial\varphi}{\partial x}\sigma_{xy} = 0, \qquad (7)$$

follow from the absence of the current flow across them. Here, S is the length of blocks in x direction and, j_y is a current density component in y direction. At their end walls $0 \le y \le d_s$, $x = \pm S/2$ we demand the uniform distribution of the x component of the current density, j_x, in a cross section of the structure,

$$j_x = \frac{\partial\varphi}{\partial x}\sigma_{xx} + \frac{\partial\varphi}{\partial y}\sigma_{xy} = \frac{I}{d_s w}. \qquad (8)$$

Here, I is the magnitude of an injection current. The last condition is rather natural even for anisotropic materials since in the absence of GB, that is for an uniform single-domain film, the boundary problem (1), (7), (8) has a trivial solution

$$\varphi = \frac{I(\sigma_{yy}x - \sigma_{xy}y)}{d_s w\sigma_c\sigma_a}. \qquad (9)$$

This solution says that the current tends to be distributed homogeneously across an anisotropic film ($j_x = I/d_s w$, $j_y = 0$) at the distances, which are sufficiently far from the current injection electrodes.

The boundary problem (1)–(8), (5) has been solved numerically. To do this, we have adopted Finite Element Method package FreeFEM++ [39]. It follows from the calculations that the presence of grain boundaries may lead to a substantial redistribution of current over the film thickness. Figure 2 shows the stream lines calculated numerically in the limit of a completely transparent GB-interface ($L \to 0$) and $\theta = 12°$. It is clear that,

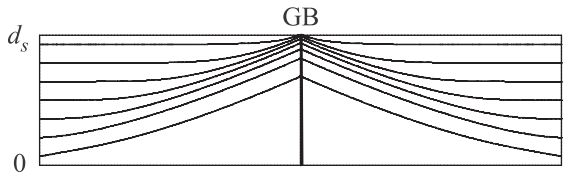

Fig. 2. The stream lines calculated numerically in the limit of fully transparent GB-interface ($L \to 0$) and $\theta = 12^\circ$

far from GB, the current starts from homogenous distribution across the film and, close to GB, tends to concentrate in the its upper part. This effect is rather trivial, if we take into account the large difference between magnitude of σ_a and σ_c, which is intrinsic for high-T_c films. The current, instead of flowing homogeneously, takes the *ab* planes on one side of GB and find the easiest way, which goes along the symmetrically located *ab* planes on the other side of the interface. The resultant spreading resistance of the part of the film, in which the current concentration takes place, is found to be less than the resistance of the same film area, containing GB, under condition of the uniform distribution of current inside it. This is illustrated in Fig. 3, where the difference between

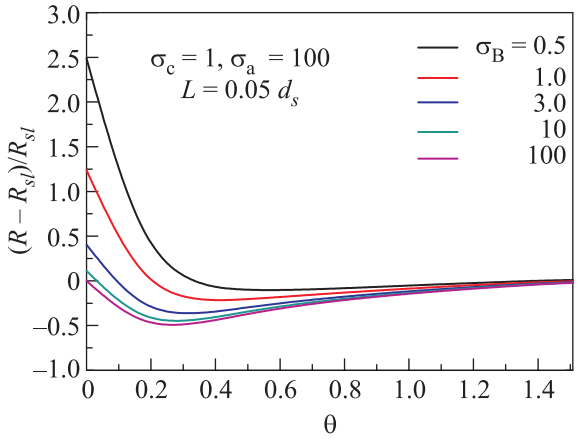

Fig. 3. The difference between the resistance of the sample with GB, R, and without it, R_{sl}, as a function of angle θ

the resistance of the sample with GB, R, and without it,

$$R_{sl} = \frac{S}{W d_s} \frac{\sigma_{yy}}{\sigma_c \sigma_a}, \qquad (10)$$

is plotted as a function of the angle θ. It is shown in Fig. 3 that, at $\theta = 12^\circ \approx 0.21$ radian, the presence of GB leads to a decrease of the resistance if $\sigma_c \lesssim \sigma_B$, while the difference $R - R_{sl}$ starts to be positive for smaller magnitudes of σ_B. It is interesting to note, that the value of $\theta = 12^\circ$ is close to the local minimum of the $R - R_{sl}$ difference as a function of θ.

The larger is the resistance $R_B = L/(W d_s \sigma_B)$ of GB itself, the smaller the effect of current concentration. This fact is illustrated in Figs. 4–6. They demon-

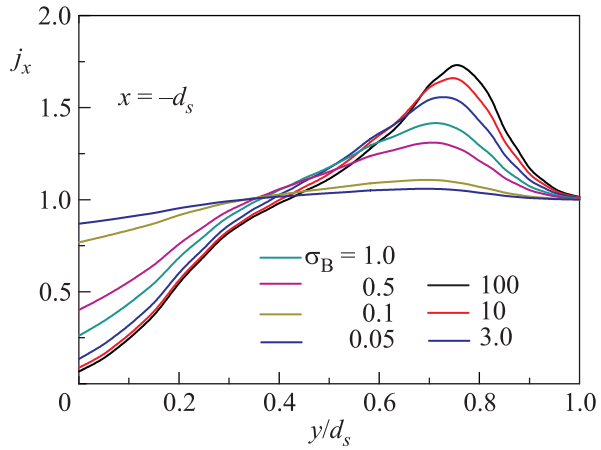

Fig. 4. Current component in the x-direction, j_x, as a function of the coordinate y calculated at the distance $x = -d_s$ from GB for $L = 0.05 d_s$, $\sigma_a = 100$, $\sigma_c = 1$, $\theta = 12^\circ$, and for a set of parameter $\sigma_B = 100, 10, 3, 1, 0.5, 0.1, 0.05$

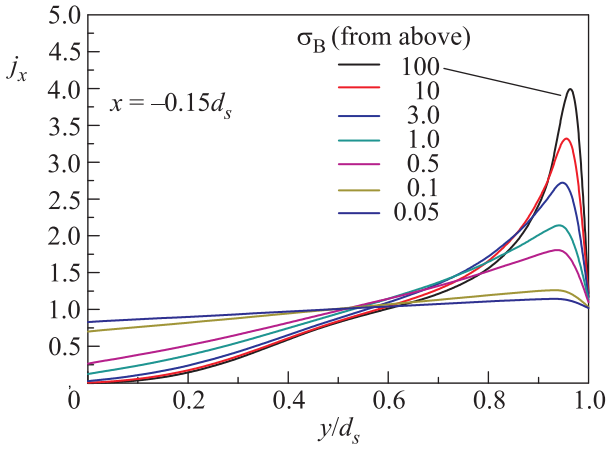

Fig. 5. Current component in the x-direction, j_x, as a function of the coordinate y calculated at the distance $x = -0.15 d_s$ from GB for $L = 0.05 d_s$, $\sigma_a = 100$, $\sigma_c = 1$, $\theta = 12^\circ$, and for a set of parameter $\sigma_B = 100$, 10, 3, 1, 0.5, 0.1, 0.05

strate the x-component of the current density, j_x, as a function of the coordinate y calculated numerically for $L = 0.05 d_s$, $\sigma_a = 100$, $\sigma_c = 1$, $\theta = 12^\circ$, and for a set of parameter σ_B from 100 to 0.05 in three cross sections of the film. As can be seen from Fig. 4 that, for $\sigma_B = \sigma_a = 100$, the current density, j_x, concentrates in the upper half part of S grain at the distance of the order of d_s from GB. The maximum value of j_x is achieved at $y \approx 0.75 d_s$ and it is approximately 20 times larger com-

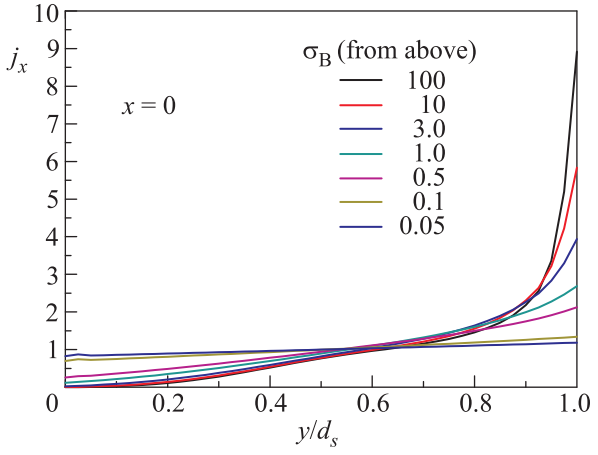

Fig. 6. Current component in the x-direction, j_x, as a function of the coordinate y calculated at GB ($x = 0$) for $L = 0.05d_s$, $\sigma_a = 100$, $\sigma_c = 1$, $\theta = 12°$, and for a set of parameter $\sigma_B = 100, 10, 3, 1, 0.5, 0.1, 0.05$

pare to the magnitude of j_x at $y = 0$. The closer is the coordinate x to GB location, the larger is this difference. The physical nature of this phenomenon lies in the generation of closed vortex currents (see Fig. 7), whose

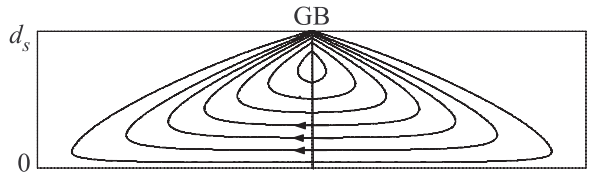

Fig. 7. The vortex current lines calculated numerically in the limit of fully transparent GB-interface ($L \to 0$) and $\theta = 12°$

existence is a direct consequence of the anisotropic nature of conductivity of high-T_c grains. It is obvious that these vortex currents generate a magnetic field. It is directed along GB perpendicular to xy-plane and located in its vicinity.

All these effects demonstrate the intensity, which is strongly depended on transport properties of GB, i.e. the smaller GB conductivity σ_B, the smaller a degree of current concentration in the upper part of GB, an intensity of vortex currents and, correspondingly, a magnitude of the magnetic field.

It is necessary to mention that the formulated boundary problem (1)–(8) can be also applied for the description of supercurrent distribution in the considered structure if under φ we mean a phase of the order parameter Δ of superconducting blocks.

This is true inside the S-grains if the magnitude of supercurrent is small enough in order to neglect the suppression of Δ, thus providing the proportionality of λ_c^{-2} and λ_a^{-2} to conductivities, σ_c and σ_a, respectively. Here, λ_c and λ_a are superconducting penetration depths in c and a directions.

At the GB, interface conditions (5), (6) are not valid and should be replaced by

$$j_x(-0, y) = j_x(+0, y) = j_c f(\chi), \qquad (11)$$

where j_c is the GB critical current density and $f(\chi)$ is a current-phase relation, that is the function, which relates the density of supercurrent across the GB to a phase difference of order parameters on both sides of GB [40]. In general, both j_c and $f(\chi)$ depend on both the intrinsic properties of GB and the form of supercurrent distribution inside the grains and must be determined selfconsistently with the solution of (1). However, if a spreading resistance, i.e. an additional part of the grain resistance due to current redistribution caused by GB, is smaller than the resistance of GB itself, then, in a first approximation, in χ we may neglect a contribution of nonlinear effects caused by the concentration of the supercurrent in the S-electrodes and consider χ as a phase jump across GB,

$$\chi = \varphi(+0, y) - \varphi(-0, y). \qquad (12)$$

If GB-junction is characterized by the simplest shape of $f(\chi) = \sin(\chi)$, then it is possible to use the condition (11) in the form

$$j_x(-0, y) = j_x(+0, y) = j_c \sin(\chi), \quad j_c = \frac{I_c}{wd_s}, \qquad (13)$$

where I_c is GB critical current.

The calculations of supercurrent distributions are in progress now and will be published elsewhere. Nevertheless, even based on the results obtained above, it is possible to conclude that anisotropy of high-T_c electrodes and corresponding redistribution of normal and supercurrent in the vicinity of GB-plays as an important role as the mechanism of current transport across the GB-junction. This conclusion is important not only for considered [100]-tilt boundaries, but also for [001]-tilt interfaces (see Fig. 1a). Note, that in the last case the degree of anisotropy is smaller in a large factor of the order of 50, but the magnetic field of vortex currents generated at the vicinity of [001]-tilt interfaces are now parallel to xy-planes, so that a [001]-tilt GB Josephson junction appears to be selfbiased by magnetic field even without any external magnetic field biasing. The situation with self-biased magnetic fields might be even more

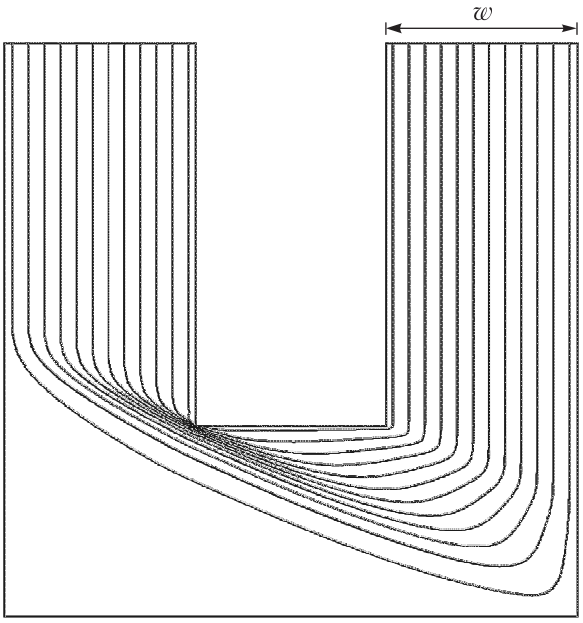

Fig. 8. The stream lines calculated numerically in the high-T_c single grain of the special shape without GB inside it, $\theta = 12^\circ$

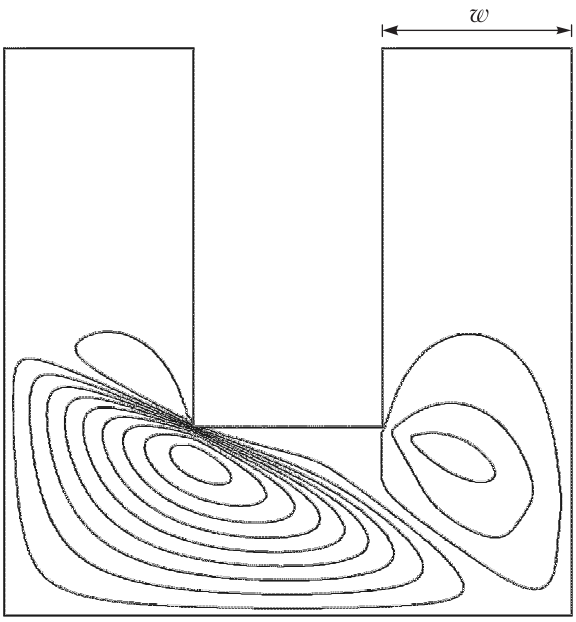

Fig. 9. The vortex current lines calculated numerically in the high-T_c single grain of the special shape without GB inside it, $\theta = 12^\circ$

complicated if twinned high-T_c thin-film electrodes are used in the [001]-tilt GB Josephson junctions. These facts should be taken into account during a data interpretations, but was completely ignored in all previous studies.

It is important to mention that the vortex currents can be nucleated not only by GB, but also by any geometrical inhomogeneity. One of the examples is demonstrated in Figs. 8, 9. A current is injected into the left part of a single grain that is identical to the left electrode of a junction presented in Fig. 1b with $\theta = 12^\circ$. The grain has the "π-shape" geometry, so that the current is outgoing from its right knee. To do this, a local vector of the current density must change its orientation with respect to crystallographical axes of the film. The vortex current nucleates just at that points, generates the local magnetic fields, which, in turn, initiates a supercurrent redistribution to screen these fields. Therefore, the anisotropy of high-T_c films is of great importance for adequate understanding of operation of any high-T_c devices.

This work has been supported by RFBR project #11-07-12023-ofi-m-2011 and in part by Swedish Institute Visby Grant #00910/2011. We are grateful to A. Kalabukhov and F. Lombardi for useful discussions.

1. H. Hilgenkamp and J. Mannhart, Rev. Mod. Phys. **74**, 485 (2002).
2. F. Tafuri and J. R. Kirtley, Rep. Prog. Phys. **68**, 2573 (2005).
3. J. H. Durrell, C.-B. Eom, A. Gurevich et al., Rep. Prog. Phys. **74**, 124511 (2011).
4. M. Putti, I. Pallecchi, E. Bellingeri et al., Supercond. Sci. Techn. **23**, 034003 (2010).
5. T. Katase, Y. Ishimaru, A. Tsukamoto et al., Nature Communications **2**, 409 (2011).
6. H. Hiramatsu, T. Katase, Y. Ishimaru et al., Materials Science and Engineering: B (2012) (to be published).
7. S. Graser, P. J. Hirschfeld, T. Kopp, et al., Nature Physics **6**, 609 (2010).
8. F. Kametani, A. Yamamoto, A. A. Polyanskii et al., Journal of the Japan Institute of Metals **74**, 444 (2010).
9. G. Deutscher, Appl. Phys. Lett. **96**, 122502 (2010).
10. U. Schwingenschlögl and C. Schuster, Phys. Rev. Lett. **102**, 227002 (2009).
11. D. C. van der Laan, T. J. Haugan, and P. N. Barnes, Phys. Rev. Lett. **103**, 027005 (2009).
12. C. Schuster and U. Schwingenschlög, J. Appl. Phys. **102**, 113720 (2007).
13. J. H. T. Ransley, S. H. Mennema, K. G. Sandeman et al., Appl. Phys. Lett. **84**, 4089 (2004).
14. G. Testa, F. Laviano, D.-J. Kang et al., Phys. Rev. B **73**, 014522 (2006).
15. G. B. Arnold and R. A. Klemm, Philosophical Magazine **86**, 2811 (2006).
16. P. M. Shadrin and Y. Y. Divin, Phys. C: **297**, 69 (1998).
17. U. Poppe, Y. Y. Divin, M. I. Faley et al., IEEE Trans. Appl. Supercond. **11**, 3768 (2001).

18. Y. Y. Divin, U. Poppe, C. L. Jia et al., Phys. C: **372–376**, 115 (2002).
19. Y. Y. Divin, I. M. Kotelyanskii, P. M. Shadrin et al., Proc. 6th European Conf. Appl. Superconductivity, Sorrento, Italy, 14–16 Sept. 2003. IOP Conf. Series **181** (ed. by A. Andreone, G. P. Pepe, R. Cristiano, and G. Masulo), IOP Publishing, Bristol, Philadelphia, 2004, p. 3112.
20. E. Stepantsov, M. Tarasov, A. Kalabukhov et al., J. Appl. Phys. **96**, 3357 (2004).
21. E. Sarnelli, G. Testa, D. Crimaldi et al., Supercond. Sci. Technol. **15**, L35 (2005).
22. I. V. Borisenko, I. M. Kotelyanski, A. V. Shadrin et al., IEEE Tran. Appl. Supercond. **15**, 165 (2005).
23. A. Ogawa, T. Sugano, H. Wakana et al., J. Appl. Phys. **99**, 123907 (2006).
24. M. V. Liatti, U. Poppe, and Y. Y. Divin, Appl. Phys. Lett. **88**, 152504 (2006).
25. Y. Y. Divin, M. V. Liatti, D. A. Tkachev, and U. Poppe, Physica C: **460–462**, 1270 (2007).
26. B. F. Logan, S. O. Rice, and R. F. Wick, J. Appl. Phys. **42**, 2975 (1971).
27. N. Toyota, H. Nakatsuji, K. Noto et al., J. Low Temp. Phys. **25**, 485 (1976).
28. R. Busch, G. Ries, H. Werthner et al., Phys. Rev. Lett. **69**, 522 (1992).
29. Y. M. Wan, T. R. Lemberger, S. E. Hebboul, and J. C. Garland, Phys. Rev. B **54**, 3602 (1996).
30. G. A. Levin, J. Appl. Phys. **81**, 714 (1997).
31. J. L. González, J. S. Espinoza Ortiz, and E. Baggio-Saitovitch, Physica C **315**, 271 (1999).
32. K. Nakao, Yu. Eltsev, J. G. Wen et al., Physica C **322**, 79 (1999).
33. S. Sarti, M. Esposito, R. Fastampa et al., Physica C **341-348**, 1915 (2000).
34. M. Esposito, L. Muzzi, S. Sarti et al., J. Appl. Phys. **88**, 2724 (2000).
35. A. Nader, Supercond. Sci. Techn. **14**, 557 (2001).
36. E. J. Zimney, G. H. B. Dommett, R. S. Ruoff, and D. A. Dikin, Measurement Science and Technology **18**, 2067 (2007).
37. J. R. Fletcher, P. J. King, and R. G. Ormson, Phys. Rev. Lett. **79**, 2522 (1997).
38. T. A. Friedmann, M. W. Rabin, J. Giapintzakis et al., Phys. Rev. B **42**, 6217 (1990).
39. http://www.freefem.org/ff++
40. A. A. Golubov, M. Yu. Kupriyanov, and E. Il'ichev, Rev. Mod. Phys. **76**, 411 (2004).